J Biomol NMR (2007) 37:321–328
DOI 10.1007/s10858-006-9129-3

NMR STRUCTURE NOTE

Solution structure of the twelfth cysteine-rich ligand-binding repeat in rat megalin

Christian A. Wolf · Felician Dancea · Meichen Shi · Veronika Bade-Noskova · Heinz Rüterjans · Dontscho Kerjaschki · Christian Lücke

Received: 27 September 2006 / Accepted: 23 November 2006 / Published online: 24 January 2007

Abstract Megalin, an approx. 600 kDa transmembrane glycoprotein that acts as multi-ligand transporter, is a member of the low density lipoprotein receptor gene family. Several cysteine-rich repeats, each consisting of about 40 residues, are responsible for the multispecific binding of ligands. The solution structure of the twelfth cysteine-rich ligand-binding repeat with class A motif found in megalin features two short β-strands and two helical turns, yielding the typical fold with a I–III, II–V and IV–VI disulfide bridge connectivity pattern and a calcium coordination site at the C-terminal end. The resulting differences in electrostatic surface potential compared to other ligand-binding modules of this gene family, however, may be responsible for the functional divergence.

Keywords Low density lipoprotein receptor · LDLR gene family · Cysteine-rich repeat · Ligand-binding domain · Calcium cage

Abbreviations

GSH	reduced glutathione
GSSG	oxidized glutathione
GST	glutathione S-transferase
LDL	low density lipoprotein
LDLR	low density lipoprotein receptor
LRP	LDLR-related protein
Meg-A12	megalin cysteine-rich ligand-binding repeat number 12 with class A motif
NOESY	nuclear Overhauser enhancement spectroscopy
RAP	receptor associated protein
RMSD	root-mean-square deviation
TEV	tobacco etch virus
TOCSY	total correlation spectroscopy
VLDL	very low density lipoprotein

C. A. Wolf · F. Dancea · M. Shi · V. Bade-Noskova · H. Rüterjans · C. Lücke
Institute of Biophysical Chemistry, Center for Biomolecular Magnetic Resonance, J.W. Goethe-University of Frankfurt, 60439 Frankfurt, Germany

D. Kerjaschki
Department of Pathology, Medical University of Vienna, Allgemeines Krankenhaus, 1090 Vienna, Austria

C. Lücke (✉)
Max Planck Research Unit for Enzymology of Protein Folding, Weinbergweg 22, 06120 Halle/Saale, Germany
e-mail: luecke@enzyme-halle.mpg.de

Present Address:
F. Dancea
CR UK Institute for Cancer Studies, University of Birmingham, Vincent Drive, Birmingham 15 2TT, UK

Biological context

Megalin, a multispecific receptor that is abundantly expressed in kidney, was first identified as the antigen responsible for the formation of immune deposits in glomerular membranous nephritis (see Christensen and Birn 2002 and refs. therein). Because of its very high molecular weight (~600 kDa) the receptor was named megalin (see Christensen and Birn 2002 and refs. therein). Subsequently, it was found that megalin is responsible for the clearance of a large number of

different substances from the glomerular filtrate in the proximal tubulus via endocytosis.

To date more than 30 proteins and other molecules that are affected by the presence of megalin have been identified; they exhibit an extreme diversity in structure, function and size. Beside hemoglobin and myoglobin, these molecules include numerous plasma proteins like insulin, vitamin binding proteins, lipoproteins, lipases, and protease/inhibitor complexes, as well as the cell surface-associated protein cubilin and pharmaceuticals like aminoglycosides. Some of the substances that are reabsorbed in the proximal tubulus, like vitamin D binding protein, represent physiologically essential molecules whose loss due to increased excretion would lead to deficiency diseases. The significance of this transport into the cell was demonstrated by the study of megalin-deficient mice, where the absence of the receptor resulted in an inability to retrieve the steroid, subsequently causing urinary loss (see Christensen and Birn 2002 and refs. therein).

The megalin ligands can be divided into two groups: (i) molecules that show affinity only to megalin and (ii) molecules that possess an additional affinity to cubilin. Cubilin is a 460 kDa membrane-associated protein that is colocated with megalin. In contrast to megalin, cubilin lacks both a transmembrane and a cytoplasmic domain. It was furthermore found that cubilin-mediated endocytosis is dependent on megalin; as a consequence, a two-receptor model has been proposed, suggesting that the cubilin-bound ligand associates to megalin to be transferred into the cell (see Christensen and Birn 2002 and refs. therein). Nevertheless, the physiological function of this co-receptor remains undetermined, thus making megalin of primary interest for further investigations.

Megalin is a member of the low-density lipoprotein receptor (LDLR) gene family. Two proteins have been found to be recognized by all members of this family: apolipoprotein E and the receptor-associated protein (RAP), which represents a chaperone required for the biosynthesis of these receptors (see Christensen and Birn 2002 and refs. therein). RAP was used in all the megalin binding studies, because it can efficiently compete with all presently known megalin ligands (Bu 1998).

Like all receptors of the LDLR family, megalin is a transmembrane glycoprotein that contains large extracellular and comparatively short intracellular domains. Four distinct structural motifs have been identified for all family members: (i) cysteine-rich complement-type repeats, (ii) EGF precursor-like repeats separated by spacer regions that include a YWTD tetrapeptide motif, (iii) a hydrophobic transmembrane domain, and (iv) a cytoplasmic domain containing a coated-pit internalization signal. These structural units are responsible for the behavior of megalin as a multi-ligand transporter. Different studies have identified the cysteine-rich repeats as essential for the binding of ligands (Russell et al. 1989; Fass et al. 1997). Structural investigations revealed that these putative ligand-binding domains share some significant conformational features: each repeat, consisting of about 40 amino acids, contains (i) six cysteine residues forming three disulfide bridges and (ii) a D-X-S-D-E sequence at the C-terminal end that takes part in a calcium cage. The connectivity pattern of the disulfide bridges (i.e. I–III, II–V and IV–VI) is the same in all modules (Bieri et al. 1998). In megalin, these cysteine-rich repeats are grouped in 4 distinct clusters containing 7, 8, 10 and 11 ligand-binding modules, respectively.

Although the basic structural organization is well described for the LDLR family, the extracellular part of the receptor conformation has been determined on the molecular level only for the low-density lipoprotein (LDL) receptor and parts of the LDLR-related protein (LRP). These structural investigations revealed that the topological features of the ligand-binding repeats in these receptors display a high diversity despite the overall similarity of the receptors (Daly et al. 1995a, b; Fass et al. 1997; Huang et al. 1999; North and Blacklow 2000; Dolmer et al. 2000; Simonovic et al. 2001). In contrast to megalin, the ligand-binding domain of the LDL receptor has been studied extensively (Russell et al. 1989): using site-directed mutagenesis, it was shown that cysteine-rich repeat number 5 plays a crucial role in the binding of LDLs as well as very low-density lipoproteins such as β-VLDL. In the case of LRP, only three cysteine-rich repeats have been studied to date, evidencing the same characteristic structural features as described above.

The ligand-binding units of this receptor family are connected by short but highly flexible linker segments, providing them a significant motional freedom. In addition, this inherent flexibility within the receptors may allow the ligand-binding repeats to adjust their relative positions in order to allow binding of a large variety of structurally dissimilar ligands (Russell et al. 1989).

Initial investigations of the megalin structure identified the second cluster of ligand-binding repeats as the antigenic epitope responsible for Heymann nephritis, an autoimmune disease in rats that represents an animal model of human glomerular membranous nephritis (Saito et al. 1996). In subsequent studies, the site of antibody interaction could be limited to amino acids 1111–1210 of rat megalin (see Christensen and Birn 2002 and refs. therein); this particular sequence contributes to the organization of the cysteine-rich repeats A10, A11, and A12,

constituting a significant part of the second cluster of ligand-binding repeats. Further investigations will be necessary to reveal detailed information about the discrete binding site(s) in order to understand all the different functions of megalin. Based on this knowledge it could become possible to develop specific strategies to inhibit the uptake of ligands in case of pathological processes (e.g. extreme myoglobin uptake leading to renal failure in case of rhabdomyolysis).

As previous studies have demonstrated that the megalin cysteine-rich ligand-binding repeat number 12 with class A motif (Meg-A12) seems to be involved in a large number of physiological processes, we chose this particular module as starting point of our structural investigation. Hence, the primary aim of the present study was the identification of unique structural features that may be responsible for the specific ligand interaction(s) of Meg-A12 in comparison to other cysteine-rich repeats.

Methods and results

Expression and purification

The rat kidney cDNA cassette encoding amino acid residues 1185–1229 of megalin (i.e. the cysteine-rich ligand-binding repeat number 12 plus 4 additional terminal residues belonging to the adjacent linker segments) was prepared by reverse transcription of the total isolated RNA with random primers. Next, for PCR amplification of the cDNA fragment, the primers Meg-up (5′-c gcc atg gtg tta aac tgt acg agt gcc cag-3′) and Meg-low (5′-cg aag ctt tta gcc ggg agg cct ggg gca gcc-3′) were used. In addition, both primers included restriction sites (*Nco*I in the forward and *Hind*III in the backward direction) to facilitate cloning into the polylinker site of the pKM263 vector (Melcher 2000). Subcloning of the resulting insert into the pKM263 vector yielded the plasmid pPM1, which served to express the cysteine-rich ligand-binding repeat Meg-A12 with N-terminal $(His)_6$-tag, GST-tag and TEV-protease cleavage site. The correct construction of the carrier vector was confirmed by restriction analysis (*Eco*RV for negative control and *Kpn*I for positive control) and DNA sequencing; both methods produced consistent results.

The soluble fusion protein $(His)_6$—GST—Meg-A12 was expressed in *E. coli* BL21 CodonPlus (DE3)-RP cells (Stratagene, La Jolla, CA, USA). The cells were grown in LB medium at 37°C to an $OD_{600} = 0.7$ before expression was induced with 0.4 mM isopropyl-β-D-thiogalactopyranoside. Six hours later the cells were harvested. For lysis, the cells were treated with lysozyme and Benzonase® (Merck, Darmstadt, Germany) followed by sonification. The $(His)_6$—GST—Meg-A12 fusion protein was extracted from the filtered supernatant by affinity chromatography using a Glutathione-Sepharose column (Amersham Pharmacia Biotech, Piscataway, NJ, USA). Subsequent digestion with $(His)_7$-TEV-protease in 50 mM Tris buffer (pH 7.4) containing 1 mM GSSG, 10 mM GSH and 5 mM $CaCl_2$ yielded the cysteine-rich ligand-binding repeat with three additional N-terminal residues (Gly1182–Ala1183–Met1184). Meg-A12 was further purified using a Ni^{2+}-chelate column (Amersham Pharmacia Biotech, Piscataway, NJ, USA) to remove the $(His)_6$-GST fragment as well as the $(His)_7$-TEV-protease. Final purification was achieved by size-exclusion chromatography using a Superdex-Peptide column (Amersham Pharmacia Biotech, Piscataway, NJ, USA). Analysis of the sample by MALDI-TOF revealed the correct molecular weight of 5092.67 Da. Correct folding of the isolated protein could be demonstrated by reverse-phase HPLC, as previously described (Bieri et al. 1998; Atkins et al. 1998). The purified protein was stored in lyophilized form.

NMR measurements

The NMR sample was prepared by dissolving Meg-A12 (1.5 mM) in 10 mM $CaCl_2$ at pH 5.5. A Bruker (Rheinstetten, Germany) DMX600 spectrometer, operating at 600.13 MHz proton resonance frequency and equipped with a 5 mm inverse triple-resonance probe that had XYZ-gradient capability, was used to carry out all NMR experiments. The NMR spectra were collected at 25°C in a phase-sensitive mode, implementing time-proportional phase incrementation for quadrature detection. The proton chemical shift values were referenced to internal 2,2-dimethyl-2-silapentane-5-sulfonate (Cambridge Isotope Laboratories, Andover, MA, USA) in order to ensure consistency among all spectra (Wishart et al. 1995). Both in the one- (1D) and two-dimensional (2D) experiments, the water signal was suppressed by selective presaturation during the relaxation delay, with the carrier placed in the center of the spectrum on the water resonance. The 2D $^1H/^1H$-TOCSY (spinlock time of either 6.1 or 80 ms) and 2D $^1H/^1H$-NOESY (mixing time of either 100 or 200 ms) spectra were acquired with 7788.2 Hz spectral width and 2048×512 data points.

All spectra were processed and analyzed on a Silicon Graphics O2 workstation using the XWINNMR 2.6 software package (Bruker, Rheinstetten, Germany). A 90° phase-shifted squared sine-bell function was used

for apodization in all dimensions. Polynomial base-line correction was applied to the processed spectra wherever necessary. The final 2D matrices consisted of 2048 × 2048 real data points. Peak picking and data analysis of the transformed spectra were performed using the AURELIA 2.5.9 software package (Bruker, Rheinstetten, Germany).

Structure determination

The sequence-specific chemical shift assignment of the ^{1}H resonances was performed according to the classical assignment strategy (Wüthrich 1986). As a consequence, the complete sequence-specific assignment of all non-labile proton resonances was obtained based on homonuclear TOCSY (see Fig. 1) and NOESY measurements and has been deposited in the BioMagResBank database under accession number BMRB-7263.

NOESY cross-peak volumes were analyzed in NMRView (Johnson and Blevins 1994). The initial NOE table containing 1307 cross-peaks with multiple assignment possibilities was refined in 8 cycles of iterative NOE assignment and structure calculations using the program ARIA 1.2 (Linge et al. 2003). In each iteration, 30 structures were calculated and the energetically 10 best models were used to interpret the NOEs in each subsequent cycle. The NOE assignment table together with the list of rejected NOEs (due to the internal violation analysis scheme of ARIA) were checked and corrected manually. Analysis of the resulting three-dimensional fold revealed that the NOE data supported the predicted disulfide bridge connectivities (i.e. I–III, II–V and IV–VI) (Bieri et al. 1998), which were subsequently introduced as unambiguous structural data.

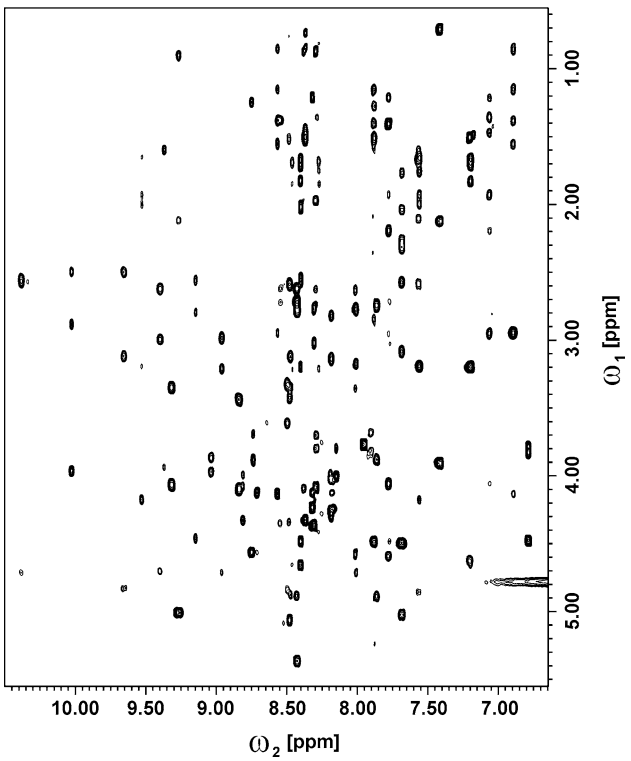

Fig. 1 Amide region of Meg-A12 in a ^{1}H/^{1}H-TOCSY spectrum collected at 25°C (600.13 MHz proton resonance frequency; 80 ms spinlock time; 10 mM $CaCl_2$ at pH 5.5)

The ARIA calculations and the additional manual refinements led to 606 non-redundant NOE distance restraints comprising 575 unambiguous and 31 ambiguous assignments (Table 1). Non-specifically assigned prochiral groups were treated with the floating chirality procedure of ARIA (Linge et al. 2003). The resulting list of NOE distance restraints was subjected to a final run of structure calculations where 200 structures were calculated using the simulated annealing protocol of ARIA. At this stage of the structure determination, a calcium atom, which is essential for the structural integrity of the module (Atkins et al. 1998), was introduced together with four artificial distance restraints of 2.5 Å each between Ca^{2+} and the $O^{\delta 2}$ respectively $O^{\varepsilon 2}$ side-chain oxygen atoms of Asp1209, Asp1213, Asp1219 and Glu1220, which had formed a cluster of acidic residues in the C-terminal lobe. The resulting 20 lowest-energy models were refined in explicit solvent (i.e. water) using a force field that accounts for electrostatic and van der Waals interactions (Linge et al. 2003). Table 1 contains the structural statistics of the final ensemble of 20 NMR structures.

Structural features of Meg-A12

The solution structure of Meg-A12 was determined based on 606 NOE-derived distance restraints. The atomic coordinates have been deposited in the RCSB database under accession number 2I1P. Figure 2A shows a superposition of the Meg-A12 core region (Cys1188–Cys1223), representing the final ensemble of 20 energy-minimized conformers. In analogy to cysteine-rich ligand-binding repeats from other receptors of the LDLR gene family (Bieri et al. 1998), it could be shown that Meg-A12 possesses the same characteristic disulfide-bridge pattern: the first bridge connects Cys1188 and Cys1201, the second Cys1195 and Cys1214, and the third Cys1208 and Cys1223. Moreover, four carboxylate side-chains (belonging to residues Asp1209, Asp1213, Asp1219 and Glu1220) together with two backbone oxygens (Tyr1206 and Val1211) form an octahedral calcium coordination site as typically found in the C-terminal lobe of these

Table 1 Structural statistics of the final 20 water-refined Meg-A12 conformers

NOE-derived distance restraints	606
Intraresidual ($i = j$)	293
Sequential ($\|i - j\| = 1$)	128
Medium-range ($1 < \|i - j\| \leq 4$)	71
Long-range ($\|i - j\| > 4$)	83
Ambiguous	31
Ca^{2+} distance restraints	4
Rms deviation from distance restraints[a] (Å)	0.013 ± 0.001
Rms deviation from covalent geometry[a]	
Bond lengths (Å)	0.004 ± 0.000
Angles (deg.)	0.483 ± 0.028
Impropers (deg.)	1.315 ± 0.130
Ramachandran plot[b] (%)	
Most favored regions	83.0
Additionally allowed regions	16.2
Generously allowed regions	0.8
Disallowed regions	0.0
RMSD of the Meg-A12 NMR ensemble[c] (Å)	
Backbone atoms	0.57 ± 0.11
All heavy atoms	1.02 ± 0.12
RMSD between Meg-A12 and other modules[d] (Å)	
PDB ID code 1AJJ (5–13, 16–39)	1.30 ± 0.16
PDB ID code 1D2J (215–223, 226–249)	1.68 ± 0.19
PDB ID code 1F8Z (3–11, 14–37)	1.51 ± 0.15
PDB ID code 1N7D (215–223, 226–249)	1.78 ± 0.13
PDB ID code 1F5Y (49–57, 62–85)	1.50 ± 0.16
PDB ID code 1CR8 (6–14, 18–41)	1.53 ± 0.13
PDB ID code 1LDR (5–13, 18–41)	2.21 ± 0.16
PDB ID code 1V9U (113–121, 126–149)	1.74 ± 0.12

[a] Evaluated by ARIA

[b] Calculated for residues Cys1188–Cys1223 with Procheck-NMR (Laskowski et al. 1996)

[c] Average RMSD from the mean structure calculated for residues Cys1188–Cys1223

[d] Average backbone RMSD for residues Cys1188–Ala1196 and Ser1200–Cys1223 compared to homologous modules (corresponding residue numbers in parentheses) that showed a PSI-BLAST score larger than 30 and an identical disulfide-bridge pattern

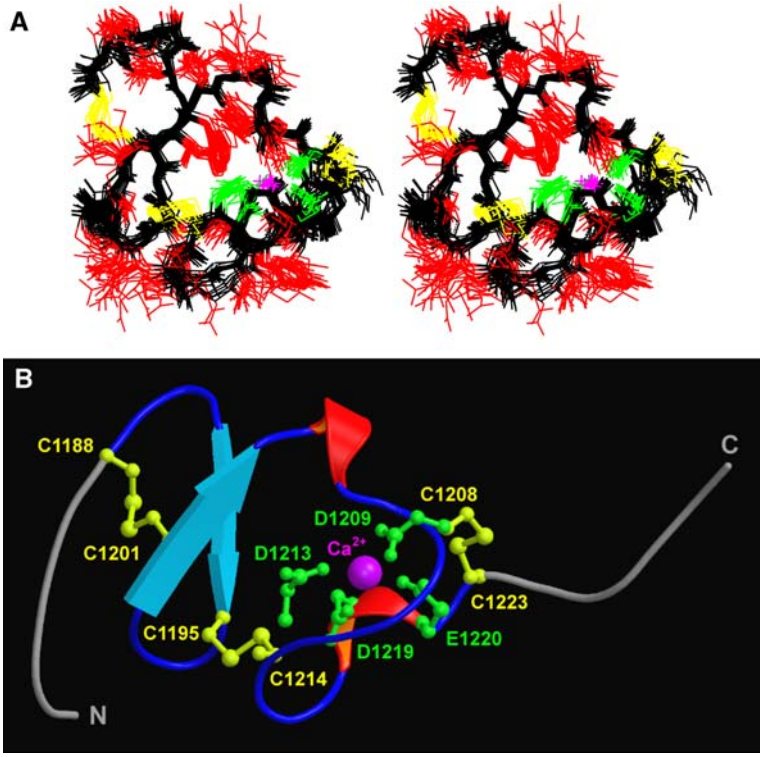

Fig. 2 (**A**) Stereo view of the 20 selected Meg-A12 conformers. Only the core region (Cys1188–Cys1223) is shown, since the remaining N- and C-terminal residues are completely disordered. The overall fold is indicated by the protein backbone (black), with side-chains colored in either red, yellow (disulfide bridges) or green (calcium cage). The Ca^{2+} atom is shown in magenta. (**B**) Ribbon diagram of the Meg-A12 structure displaying the secondary structure elements. The helical segments are colored in red, whereas β-strands are represented as arrows (cyan). The disulfide bridges and the calcium cage are shown in the same color-code as in the upper panel

lipid-binding modules (North and Blacklow 2000; Atkins et al. 1998; Fass et al. 1997).

The N- and C-terminal residues (i.e., Gly1182–Asn1187 and Pro1224–Gly1229, respectively) were found to be completely randomly organized, whereas the core region of Meg-A12, i.e. Cys1188–Cys1223, is well defined with an average backbone root-mean-square deviation (RMSD) of 0.57 ± 0.11 Å from the

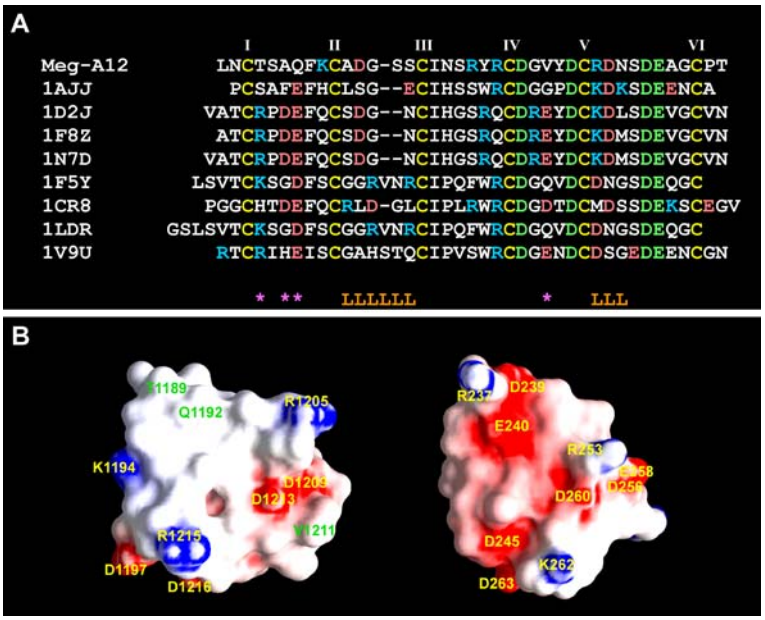

Fig. 3 (**A**) Sequence comparison of the Meg-A12 core region with the related cysteine-rich repeats that have been structurally resolved to date. The six highly conserved cysteine residues with the disulfide connectivity pattern I–III, II–V and IV–VI are indicated in yellow color and with Roman numerals on top. Also highly conserved are the acidic residues in green color, which coordinate the calcium ion. Red and blue color indicates all other acidic and basic residues, respectively. The two adjacent loop segments with increased conformational variability and varying charge distributions are marked with the letter L in the bottom row; other residues where differences in the electrostatics are found between Meg-A12 and the related LDLR domains are indicated by an asterisk. (**B**) Surface potential maps of Meg-A12 (left) and the sixth ligand-binding module of human LDLR (PDB ID code 1F8Z; right). Both molecules are shown in the same orientation after superposition of the backbone atoms. In this view, the calcium ion is located just below the surface on the right side, i.e. between Asp1209 and Asp1213 in Meg-A12, respectively between Asp256 and Asp260 in human LDLR. The variable loop segments are found at the lower left edge. Very pronounced electrostatic differences are oberved in the upper half of this molecule face, where the N-terminal segment of the Meg-A12 core region is less acidic than the related LDLR modules. Surface coloring indicates the electrostatic potentials calculated by GRASP (Nicholls et al. 1991) within boundary values of –10 kT (intense red) to +10 kT (intense blue)

mean structure (Table 1). The best defined backbone segment, however, was identified between Gln1192 and Ala1221 (average backbone RMSD from mean structure of 0.47 ± 0.13 Å). The distribution of φ- and ψ-angles in the Ramachandran plot shows that all non-glycine/non-proline residues in the Meg-A12 core region are located within the allowed conformational space (Table 1).

The Meg-A12 structure (Fig. 2B) displays two helical turns at the segments Ser1204–Tyr1206 and Ser1218–Glu1220. In addition, two short β-strands span from Gln1192 to Cys1195 and from Ser1200 to Asn1203, forming an antiparallel β-sheet structure. This β-sheet is defined by interstrand NOE connectivities between Phe1193 H^N and Ile1202 H^N, Ile1202 H^N and Lys1194 H^α, Lys1194 H^α and Cys1201 H^α, Cys1201 H^α and Cys1195 H^N as well as Cys1195 H^N and Ser1200 H^N. Consequently, hydrogen bonds occur between Phe1193 H^N and Ile1202 O, Phe1193 O and Ile1202 H^N as well as Ser1200 O and Cys1195 H^N.

Discussion and conclusions

LDL-class A modules are currently found in more than 100 proteins, which do not all belong to the LDLR gene family. Moreover, they were also identified in the complement cascade. This fact shows their widespread appearance and biological importance. Nevertheless there exist only very few structural investigations on megalin to date.

Here we show that Meg-A12, as a member of the LDLR family, possesses a fold typical for modules with class A motif. The core region of the Meg-A12 structure, i.e. all residues from the first to the last cysteine, is well defined as indicated by the backbone RMSD and the Ramachandran plot distribution. Only the loop comprising residues Ala1196–Ser1200 as well as the spacially neighbouring segment Arg1215–Asn1217 both show an increased conformational variability, possibly indicating a higher structural flexibility that could allow the binding of different ligand types.

In particular the loop Ala1196–Ser1200 between the second and third cysteine residue is remarkable as it consists of five residues in Meg-A12, while the related LDLR domains usually feature either four or six residues within this segment. We have therefore excluded all but the first and last residue of this loop in the structural comparison of the Meg-A12 core region with the other structurally resolved domains (Table 1). The highest structural homology to Meg-A12 was subsequently found for the human LDLR ligand-binding module 5 (PDB ID code 1AJJ) with an average backbone RMSD of 1.30 ± 0.16 Å (Table 1).

Despite this high degree of similarity in their overall three-dimensional fold, the different modules are characterized by various binding preferences, suggesting that the electrostatic surface distribution may be another decisive feature. The acidic motifs conserved on the surface of most of the cysteine-rich repeats involved in ligand binding have been discussed in the past as an essential feature for ligand specificity (North and Blacklow 2000), since some of the physiological ligands represent basic molecules.

A comparison of the net charges shows that the core region of Meg-A12 is less acidic than most of the LDLR-derived domains. Within the segments that correspond to the two above-mentioned neighbouring loops Ala1196–Ser1200 and Arg1215–Asn1217 in Meg-A12, varying charge distributions occur throughout the different cysteine-rich repeats (Fig. 3A), possibly representing an additional factor for functional diversity. More pronounced, however, are the charge differences between Meg-A12 and the related LDLR domains in a segment between the first and the second cysteine and at a residue located between the fourth and fifth cysteine. More precisely, residue Val1211 of Meg-A12 is replaced in many LDLR modules by an acidic residue, thus rendering the protein surface even more negative at the calcium-binding site. Second, while the N-terminal segment Thr1189–Ser1190–Ala1191–Gln1192 is uncharged in Meg-A12 (as well as Meg-A10 and Meg-A11), the related LDLR domains contain a conserved acidic residue in place of Gln1192, a conserved basic residue instead of Thr1189, and quite often another acidic residue that replaces Ala1191.

Hence, in most of the related cysteine-rich repeats that have been structurally resolved to date, the face where the calcium-binding site is located displays an overall higher negative surface charge compared to Meg-A12, as shown for instance in Fig. 3B for the sixth ligand-binding module of human LDLR. This divergence in the electrostatic surface potential near the calcium-binding site may thus be the predominant feature that defines the functional differences between Meg-A12 and other ligand-binding modules of the LDLR gene family.

Acknowledgements The authors would like to thank Sigurd Krieger (Medical University of Vienna) for kindly providing the cDNA cassette of Meg-A12, Dr. Frank Bernhard (University of Frankfurt) for kindly providing $(His)_7$-TEV-protease, and Dr. Vladimir Rogov for helpful discussions. The European Large Scale Facility for Biomolecular NMR at the University of Frankfurt is acknowledged for the use of its equipment.

References

Atkins AR, Brereton IM, Kroon PA, Lee HT, Smith R (1998) Calcium is essential for the structural integrity of the cysteine-rich, ligand-binding repeat of the low-density lipoprotein receptor. Biochemistry 37:1662–1670

Bieri S, Atkins AR, Lee HT, Winzor DJ, Smith R, Kroon PA (1998) Folding, calcium binding, and structural characterization of a concatemer of the first and second ligand-binding modules of the low-density lipoprotein receptor. Biochemistry 37:10994–11002

Bu G (1998) Receptor-associated protein: a specialized chaperone and antagonist for members of the LDL receptor gene family. Curr Opin Lipidol 9:149–155

Christensen EI, Birn H (2002) Megalin and cubilin: multifunctional endocytic receptors. Nat Rev Mol Cell Biol 3:258–268

Daly NL, Scanlon MJ, Djordjevic JT, Kroon PA, Smith R (1995a) Three-dimensional structure of a cysteine-rich repeat from the low-density lipoprotein receptor. Proc Natl Acad Sci USA 92:6334–6338

Daly NL, Djordjevic JT, Kroon PA, Smith R (1995b) Three-dimensional structure of the second cysteine-rich repeat from the human low-density lipoprotein receptor. Biochemistry 34:14474–14481

Dolmer K, Huang W, Gettins PGW (2000) NMR solution structure of complement-like repeat CR3 from the low density lipoprotein receptor-related protein. Evidence for specific binding to the receptor binding domain of human α_2-macroglobulin. J Biol Chem 275:3264–3269

Fass D, Blacklow S, Kim PS, Berger JM (1997) Molecular basis of familial hypercholesterolaemia from structure of LDL receptor module. Nature 388:691–693

Huang W, Dolmer K, Gettins PGW (1999) NMR solution structure of complement-like repeat CR8 from the low density lipoprotein receptor-related protein. J Biol Chem 274:14130–14136

Johnson BA, Blevins RA (1994) NMR View: A computer program for the visualization and analysis of NMR data. J Biomol NMR 4:603–614

Laskowski RA, Rullmann JA, MacArthur MW, Kaptein R, Thornton JM (1996) AQUA and PROCHECK-NMR: programs for checking the quality of protein structures solved by NMR. J Biomol NMR 8:477–486

Linge JP, Habeck M, Rieping W, Nilges M (2003) ARIA: automated NOE assignment and NMR structure calculation. Bioinformatics 19:315–316

Melcher K (2000) A modular set of prokaryotic and eukaryotic expression vectors. Anal Biochem 277:109–120

Nicholls A, Sharp KA, Honig B (1991) Protein folding and association: insights from the interfacial and thermodynamic properties of hydrocarbons. Proteins 11:281–296

North CL, Blacklow SC (2000) Solution structure of the sixth LDL-A module of the LDL receptor. Biochemistry 39:2564–2571

Russell DW, Brown MS, Goldstein JL (1989) Different combinations of cysteine-rich repeats mediate binding of low density lipoprotein receptor to two different proteins. J Biol Chem 264:21682–21688

Saito A, Yamazaki H, Rader K, Nakatani A, Ullrich R, Kerjaschki D, Orlando RA, Farquar MG (1996) Mapping rat megalin: the second cluster of ligand binding repeats contains a 46-amino acid pathogenic epitope involved in the formation of immune deposits in Heymann nephritis. Proc Natl Acad Sci USA 93:8601–8605

Simonovic M, Dolmer K, Huang W, Strickland DK, Voltz K, Gettins PGW (2001) Calcium coordination and pH dependence of the calcium affinity of ligand-binding repeat CR7 from the LRP. Comparison with related domains from the LRP and the LDL receptor. Biochemistry 40:15127–15134

Wishart DS, Bigam CG, Yao J, Abildgaard F, Dyson HJ, Oldfield E, Markley JL, Sykes BD (1995) ^{1}H, ^{13}C and ^{15}N chemical shift referencing in biomolecular NMR. J Biomol NMR 6:135–140

Wüthrich K (1986) NMR of proteins and nucleic acids. Wiley, New York